ACCOUNTS
of chemical research

Nanoshell-Enabled Photothermal Cancer Therapy: Impending Clinical Impact

SURBHI LAL,[†,⊥] SUSAN E. CLARE,[||] AND NAOMI J. HALAS[*,†,‡,§,⊥]

[†]Department of Electrical and Computer Engineering, [‡]Department of Chemistry, [§]Department of Bioengineering, and [⊥]The Laboratory for Nanophotonics, Rice University, 6100 Main Street, Houston, Texas 77005, and [||]Department of Surgery, Indiana University School of Medicine, Indianapolis, Indiana 46202

RECEIVED ON JUNE 26, 2008

CONSPECTUS

Much of the current excitement surrounding nanoscience is directly connected to the promise of new nanoscale applications in cancer diagnostics and therapy. Because of their strongly resonant light-absorbing and light-scattering properties that depend on shape, noble metal nanoparticles provide a new and powerful tool for innovative light-based approaches.

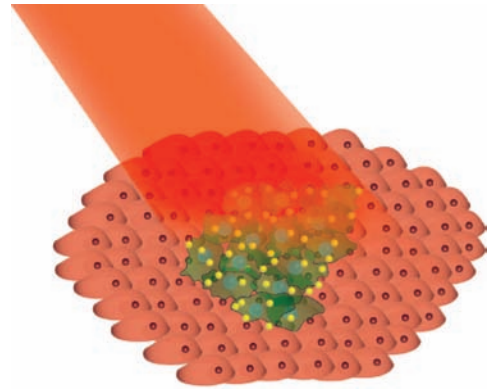

Nanoshells—spherical, dielectric core, gold shell nanoparticles—have been central to the development of photothermal cancer therapy and diagnostics for the past several years. By manipulating nanoparticle shape, researchers can tune the optical resonance of nanoshells to any wavelength of interest. At wavelengths just beyond the visible spectrum in the near-infrared, blood and tissue are maximally transmissive. When nanoshell resonances are tuned to this region of the spectrum, they become useful contrast agents in the diagnostic imaging of tumors. When illuminated, they can serve as nanoscale heat sources, photothermally inducing cell death and tumor remission. As nanoshell-based diagnostics and therapeutics move from laboratory studies to clinical trials, this Account examines the highly promising achievements of this approach in the context of the challenges of this complex disease. More broadly, these materials present a concrete example of a highly promising application of nanochemistry to a biomedical problem.

We describe the properties of nanoshells that are relevant to their preparation and use in cancer diagnostics and therapy. Specific surface chemistries are necessary for passive uptake of nanoshells into tumors and for targeting specific cell types by bioconjugate strategies. We also describe the photothermal temperature increases that can be achieved in surrogate structures known as tissue phantoms and the accuracy of models of this effect using heat transport analysis. Nanoshell-based photothermal therapy in several animal models of human tumors have produced highly promising results, and we include nanoparticle dosage information, thermal response, and tumor outcomes for these experiments.

Using immunonanoshells, infrared diagnostic imaging contrast enhancement and photothermal therapy have been integrated into a single procedure. Finally, we examine a novel "Trojan horse" strategy for nanoparticle delivery that overcomes the challenge of accessing and treating the hypoxic regions of tumors, where blood flow is minimal or nonexistent. The ability to survive hypoxia selects aggressive cells which are likely to be the source of recurrence and metastasis. Treatment of these regions has been incredibly difficult. Ultimately, we look beyond the current research and assess the next challenges as nanoshell-based photothermal cancer therapy is implemented in clinical practice.

Introduction

It is projected that a total of 1,437,180 new cancer cases and 565,650 deaths from cancer will occur in the United States in 2008,[1] accounting for one in four deaths. Since the U.S. population 65 years and older will double in the next few

Published on the Web 11/19/2008 www.pubs.acs.org/acr
10.1021/ar800150g CCC: $40.75

decades,[2] cancer diagnoses are expected to increase by 38% between 2005 and 2020.[3] While improvements in traditional cancer therapies have resulted in a continued decrease in cancer death rates since the early 1990s,[1] if we are to permanently reverse the trends reflected in these statistics and strike a decisive blow against this disease, the following critical challenges must be addressed:

1. **We need to understand the causes of cancer, so that interventions can be developed for prevention.**
2. **We must develop tools for early detection.** For example, ovarian cancer is curable if detected in its earliest stage; the 5-year survival for localized disease is 92% versus 30% for metastatic disease.[1] To address this challenge, nanotechnology may substantially increase the sensitivity and specificity of current diagnostic techniques and may enable the development of completely novel imaging modalities.
3. **We need to devise effective treatments for all stages of cancer, in particular, advanced stage metastatic disease and especially for metastatic disease in privileged sites, that is, the brain.** Much of the recent progress in cancer therapy has involved the treatment of early stage, localized disease where conventional surgical approaches followed by chemotherapy or radiation therapy provide standard protocols. However, the majority of cancer diagnoses are for more advanced stages of the disease. For example, 70% of ovarian cancers are already metastatic when diagnosed.[1] As technology advances are developed for cancer therapy, it is important that strategies for all stages of the disease are developed, in particular for those cases where no surgical option currently exists.

Much of the current excitement surrounding nanoscience and nanotechnology is focused on the potential use of chemically synthesized and functionalized nanoparticles designed specifically for biomedical applications. Indeed, perhaps the greatest promise of impact for nanochemistry is in nanoparticle-based approaches designed to address the specific diagnostic and therapeutic challenges of cancer. While many approaches are being developed for nanotechnology-enabled cancer diagnostics and therapeutics, a remarkably promising strategy involves the combination of noble metal nanoparticles and light. The uniquely vivid colors of metallic nanoparticles such as gold or silver are a result of their strong optical resonances.[4] When illuminated by light, metal nanoparticles support coherent oscillations of their valence electrons known as surface plasmons. The plasmon resonance wavelength depends strongly on the shape and size of the metal nanoparticle, as well as the type of metal and its local environment.[5] There is very strong enhancement of absorption or scattering at the plasmon resonant wavelength of the nanoparticle, depending on nanoparticle size: smaller plasmonic nanoparticles are better absorbers, and increasing size increases the nanoparticle scattering cross section.[6] Fortuitously, nanoparticles in the 100 nm diameter size range can possess both strong resonant absorption and scattering characteristics. The resonant absorption properties of metallic nanoparticles result in strong, highly localized photothermal heating upon laser illumination, an effect that can be exploited to induce cancer cell death and tumor remission. The light scattering properties can be utilized for contrast enhancement in bioimaging. These two inherent properties of nanoparticles can be combined for integrated diagnostic imaging and therapeutics.

Nanoshells, spherical nanoparticles consisting of a dielectric (silica) core and a metallic shell layer, provide a systematic approach to "nanoengineering" the optical resonance wavelength of a metallic nanoparticle.[7] By variation of the relative size of the inner and outer shell layer, the plasmon resonance of a nanoshell can be "tuned" to any wavelength desired across a large region of the visible and infrared spectrum.[5] In particular, the optical resonance of nanoshells can be tuned to the near-infrared between 700−1100 nm in wavelength, where water absorption is minimal and blood and tissue are maximally transmissive.[8] Nanoshells with resonances in this region of the spectrum can serve as strong absorbers or scatterers of near-infrared light as desired, determined by their size. In this way, gold nanoshells combine the biocompatibility of gold nanoparticles with a new tailored infrared plasmon resonance wavelength, which enables their use *in vivo* for biomedical applications. Subsequent to the development of Au nanoshells, gold nanoparticles such as nanorods or nanocages have been developed with shape-dependent near-IR optical resonances and are also being applied to cancer therapy.[9,10]

In the past five years, nanoshell-based photothermal cancer therapy has been realized, and the transition from bench to bedside for this potentially revolutionary approach has begun. As this application transitions from initial proof-of-concept studies to clinical settings in an expanding number of research groups and hospitals, we provide a view of the current state of nanoshell-based therapeutics and diagnostics for cancer.

Nanoparticle Properties Specific to *in Vivo* Applications

Most nanoparticle-based diagnostic and therapeutic techniques rely on the accumulation of nanoparticles at the tumor site, which can occur by several different mechanisms. One approach relies on the passive accumulation of nanoparticles at the tumor site through the leaky tumor vasculature. Malignant tumors rapidly develop new vasculature to supply the expanding tumor mass. These new blood vessels are structurally abnormal and irregularly shaped with inconsistent diameters and large gaps (up to 2 μm).[11] These gaps are large enough to allow large molecules and nanoparticles in the blood stream to be taken up into the tumor. This property is referred to as the "enhanced permeability and retention (EPR) effect".[12,13] Without an appropriate surface coating, nanoparticles in the blood stream are rapidly removed from circulation, limiting their availability for tumor uptake.[14] Nanoparticles can be protected from this fate by chemically functionalizing their surfaces. In particular, attaching poly(ethylene glycol) (PEG) to the nanoparticle surface has proven to be quite successful for extending the circulation time of nanoparticles in the bloodstream and enhancing passive accumulation in tumors.[15] The thiol (−SH) moiety is a facile group for conjugation to a gold nanoparticle surface. Nanoshells coated with thiol-modified PEG (PEG-SH) are used to protect nanoshells injected into the bloodstream from being removed before they can accumulate in the tumors. Details on PEGylating nanoshells may be found in ref 16.

In addition to passive accumulation, nanoshell delivery may be directed by conjugating the nanoparticles to antibodies, proteins, or ligands specific to surface markers overexpressed by cancer cells. Many solid tumors are known to express proteins such as HER2, α_v integrin receptor, and interleukin receptor, all of which have been used to target the delivery of nanoparticles to tumor sites.[17] A successful protocol that has been used for attaching antibodies to nanoshells is using bifunctional PEG linker molecules. Antibodies such as anti-HER2 are conjugated to orthopyridyl disulfide-PEG-*n*-hydroxysuccinimide (OPSS-PEG-NHS). The resulting OPSS-PEG-antibody conjugates react with the gold surface to form a layer of PEG-antibody on the nanoshell surface.[16]

Heating Profiles

Nanoshells used in photothermal ablation of cells are designed to be highly absorbing in the NIR region of the spectrum, resulting in preferential heating upon laser illumination only in the direct vicinity of the nanoshells. Heating of the target region is controlled by both nanoshell concentration and laser power.

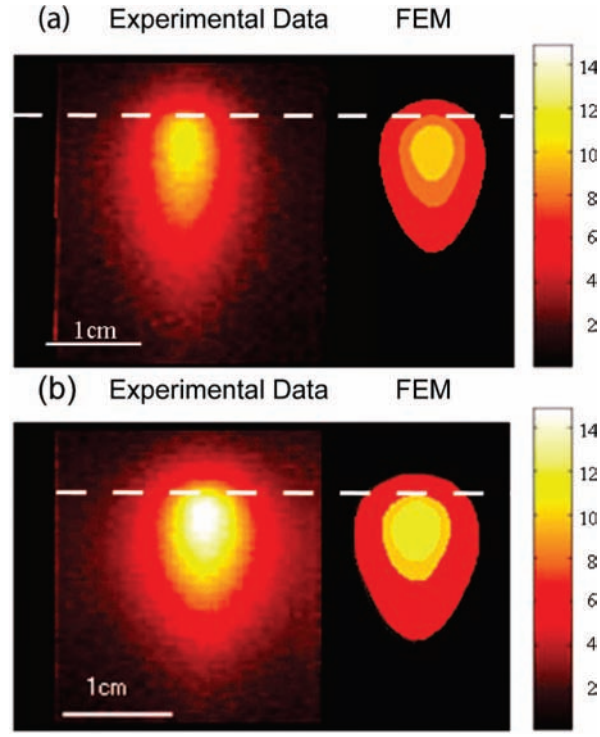

FIGURE 1. Nanoshell-based photothermal heating in (a) 0.55 OD and (b) 0.695 OD nanoshell-laden tissue phantoms consisting of a synthetic scattering medium (Lipsyn), which replicates the optical scattering properties of tissue, incorporating nanoshells for contrast enhancement and photothermal therapy. The color bar indicates the change in temperature of the tissue phantom. Dashed line indicates boundary of nanoshells in gel. Reprinted with permission from ref 18, copyright 2007 AAPM.

Elliot et al. have quantified this nanoshell−laser interaction to determine the effect of nanoshell concentration and laser power in light-induced thermal therapy.[18] Tissue phantoms (1.5% agarose gel) with 110 nm diameter nanoshells at 0.55 optical density (OD) and 180 nm diameter nanoshells at 0.695 OD were prepared. The gels were irradiated with a Diomed 15 Plus cw laser at 808 nm wavelength. The laser power was varied from 0.4 to 1.5 W, and the laser spot was maintained at ~0.5 cm. The spatiotemporal distribution of heat was measured using magnetic resonance thermal imaging, a technique based on the temperature sensitivity of the proton resonance frequency, implemented in a commercial magnetic resonance imaging (MRI) scanner. The measured temperature distribution for both sets of phantoms are shown in Figure 1. The heat distribution was simulated using a commercial finite element method (FEM) modeling package (COMSOL, Multiphysics). An overlay of the isotherms at 5, 8, and 10 °C rise

in temperature, generated by the FEM model, are shown alongside in Figure 1. The theoretical spatiotemporal distribution, the heating (cooling) profile while the nanoshell-laden phantom is irradiated by the laser, and the laser power dependence of the temperature distribution compare very well with experimentally measured quantities. This demonstrates that FEM modeling can provide quantitative agreement with the effective heating profiles obtained in nanoshell-based therapeutics and should be applicable, with appropriate modifications, to optimizing nanoshell dosages for clinical applications.

Biodistribution of Nanoshells

Neutron activation analysis (NAA) studies have been undertaken to determine optimal nanoshell accumulation times in tumors and biodistribution of nanoshells in various organs.[19] NAA is a highly sensitive technique to identify and quantify various elements in a sample and can be used to determine the quantity of gold present in tissue samples. The technique relies on the transformation of atoms to different radioisotopes following irradiation with neutrons and subsequent γ ray emission as the radioisotopes decay. The emission consists of signatures of the nuclei of the specific elements from which the γ rays are emitted.

For these studies, mice with subcutaneous tumors were injected with PEGylated nanoshells. The mice were then sacrificed at different times, and tissue samples were prepared for neutron activation analysis. γ-ray spectroscopy was carried out 4−8 days after irradiation to quantify the gold content in blood, tumor, spleen, liver, lungs, kidney, brain, bone, and muscle tissues.

The NAA data indicate that nanoshells are cleared from the blood stream in a day and are scavenged by the liver and spleen. The nanoshell concentrations in the liver and spleen continue to increase after a day and do not reach normal levels even after 28 days, the longest time point in the study. The nanoshells accumulate in the tumor and reach a maximum concentration after 24 h after which the nanoshell concentration in the tumor diminishes.

While NAA remains the standard to determine nanoshell concentrations, alternate techniques for faster determination of blood circulation times that ultimately determine accumulation in tumors are being developed. A nondestructive optical approach developed by Xie et al. utilizes dynamic light scattering (DLS) from nanoshell and Triton X-100 solutions in whole blood.[20] The Triton X-100 acts as a standard against which the scattering from the nanoshells in blood may be quantified. For *in vivo* determination of nanoshell circulation times, mice were injected with a PEGylated nanoshell solution. Fifteen microliter blood samples were taken at various time points, and a known amount of Triton X-100 solution was added to each sample. DLS measurements were performed to quantify the scattering, yielding the nanoshell concentrations. The same samples were then analyzed using NAA, where a correlation between the nanoshell concentrations obtained using these two techniques showed excellent agreement.

Nanoshell-Enabled Tumor Imaging and Therapy

Nanoshell-based photothermal therapy of cancer relies strongly on the absorption of NIR light by nanoshells and the efficient conversion of the light to heat. The nanoshells heat the tumor in which they are embedded. When a temperature increase of 30−35 °C is photothermally induced, significant cell death is observed.[21] Similarly, the diagnostic imaging of tumors at laser power levels that do not induce heating has been shown to be enhanced by using nanoshell-based contrast agents. Nanoshells designed to scatter light in the NIR physiological transparency window have been shown to act as stable contrast agents for imaging modalities such as dark field scattering,[22,23] diffuse light scattering,[24] photoacoustic tomography (PAT),[25] and optical coherence tomography (OCT).[22,26]

Nanoshell-based therapy was first demonstrated in tumors grown in mice.[21] Subcutaneous tumors were grown in mice to a size of ∼1.0 cm in diameter. PEGylated nanoshells were directly injected into the tumors under magnetic resonance imaging (MRI) guidance. Control tumors received saline injections. The tumors were subsequently exposed to NIR light, and the tumor temperature, as well as the temperature of the adjacent tissue, was monitored during and after laser irradiation. The mice were euthanized, and tumors were excised for histological evaluation. Analysis of the nanoshell-based photothermal treatment reveals tissue damage in an area of similar extent as that exposed to laser irradiation (Figure 2).

Magnetic resonance thermal imaging (MRTI) was used to monitor the temperature profile of the tumor during and after irradiation. Analysis of these temperature maps reveals an average temperature increase of 37.4 ± 6.6 °C after 4−6 min of irradiation. These temperatures were sufficient to induce irreversible tissue damage. Nanoshell-free control samples show an average temperature rise of 9.1 ± 4.7 °C, considered to be safe for cell viability.

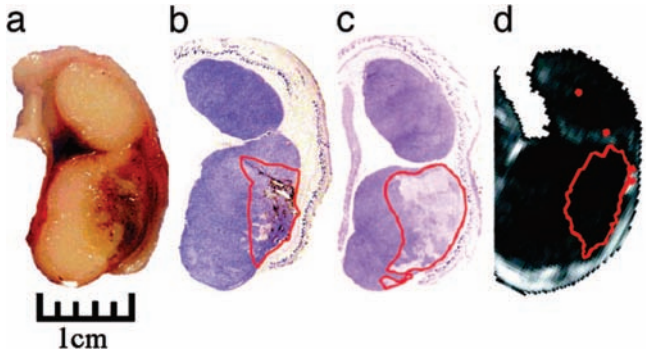

FIGURE 2. (a) Gross pathology after *in vivo* treatment with nanoshells and NIR laser reveal hemorrhaging and loss of tissue birefringence beneath the apical tissue surface. (b) Silver staining of a tissue section reveals region of localized nanoshells (red). (c) Hematoxylin/eosin staining within the same plane clearly shows tissue damage within the area occupied by nanoshells. (d) MRTI calculations reveal area of irreversible thermal damage similar to that in panel a, b, and c. Reprinted with permission from ref 21. Copyright 2003 National Academy of Sciences, U.S.A.

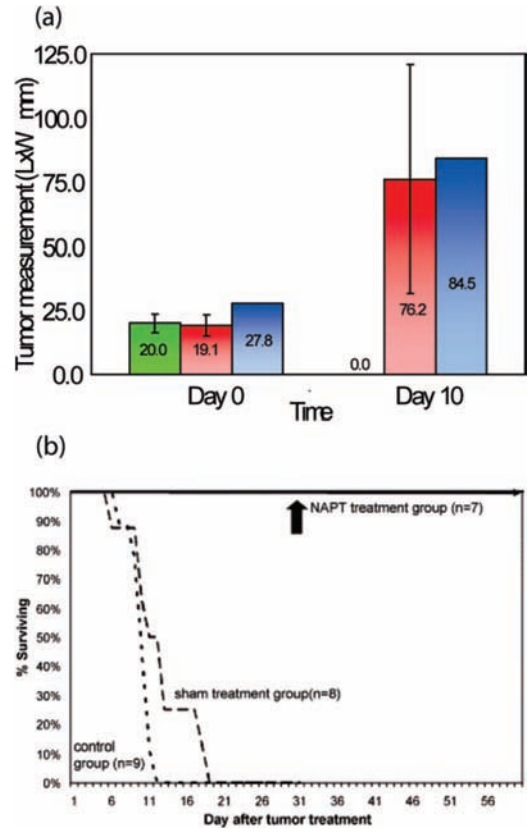

FIGURE 3. (a) Mean tumor size on treatment day and day 10 for the treatment group (green), control group (red), and sham treatment (blue). (b) Survival for first 60 days. Average survival time for the nanoshell-treated group was >60 days, control group was 10.1 days, and sham treatment group was 12.5 days. Reprinted with permission from ref 27. Copyright 2004 Elsevier.

Subsequent experiments were then conducted to determine the therapeutic efficacy and animal survival times by monitoring the tumor growth and regression over a period of 90 days.[27] In these studies, tumors were grown subcutaneously in mice, and PEGylated nanoshells were injected systemically via the tail vein, accumulating in the tumor over 6 h. The tumors were then irradiated with a diode NIR laser at a wavelength of 808 nm at a power of 4 W/cm^2 for 3 min. A sham treatment group received the same laser treatment following saline injection, and a control group received no treatment. Following this treatment, the change in tumor size over the first 10 days indicates a dramatic difference in tumor size for the three control groups (Figure 3a). In the nanoshell-treated group there was 100% resorption of the tumor at the 10 day mark. In the rest of the study, this result persisted, whereas in the sham and control groups, the tumor burden became large enough (tumor burden doubled in size corresponding to >5% body weight) that the mice were euthanized. Figure 3b is a plot of the survival statistics for the three groups of mice. At 90 days post-treatment, all mice in the treatment group were healthy and free of tumors.

The passive accumulation of nanoshells in tumors and subsequent ablation relies on a minimum accumulation of nanoshells in the tumor. Stern et al. have evaluated the effect of nanoshell concentration on tumor ablation in a human prostate cancer model in mice.[28] Tumors were grown subcutaneously. PEGylated nanoshells of two different dosages (7.0 μL/gm (low dose) and 8.5 μL/gm of body weight (high dose)) were delivered into the mice via tail vein injection. The nanoshells were allowed to accumulate for 18 h at which time the tumors were irradiated using a Diomed NIR laser at 810 nm for 3 min. Tumor size was measured for 21 days. In the low dose group, only partial tumor ablation was achieved. Nine of the ten tumors showed arrested growth (mean volume 49.2 mm^3 from a baseline of 41.6 mm^3), as opposed to the control sample where the tumor burden tripled in 21 days (126.4 mm^3 from a baseline of 43.5 mm^3). Histologically the tumors showed partial ablation with patchy areas of normal tumor cells. In the high dose treatment group, at 21 days complete tumor deletion was observed (Figure 4). Histological evaluation also confirmed complete tumor necrosis for this dosage. In the high dose treated group, a well circumscribed eschar formed over the laser treated region by day 1. This eschar fell off by day 21 revealing normal healthy skin. The control samples that did not receive any nanoshells did not form an eschar over the laser-treated areas. In the high dose group, the average temperature achieved was 65.4 °C, which is known to be effective in thermal ablation therapy.

FIGURE 4. Photothermal tumor ablation: (A) tumor before treatment; (B) complete ablation of tumor in the high dose group. The eschar formed over the laser-treated region fell off by day 21 exposing healthy skin. Figure reproduced with permission from ref 28. Copyright 2008 Elsevier.

Nanoshells as Contrast Agents

In addition to being strong near-IR absorbers, nanoshells can be strong scatterers of NIR light. This opens up the potential for diagnostic imaging of tumors for early detection. Optical techniques have the advantage of being minimally invasive and offer high resolution images using biocompatible nonphotobleaching nanoshells to improve contrast. Compared with molecular contrast agents such as indocyanine green, nanoshells have far larger scattering cross sections and a tunable optical response over a wide wavelength range. Nanoshells synthesized with high scattering cross sections have been used as contrast agents in numerous imaging modalities,[25,26,29,30] enhancing the sensitivity of these imaging techniques.

Loo et al. have demonstrated the use of scattering nanoshells targeted with anti-HER2 as a contrast agent in dark-field microscopy. HER2 positive SK Br3 and HER2 negative MCF7 cell cultures were incubated with anti-HER2 and anti-IgG immunonanoshells.[29] After 1 h, the cells were rinsed and visualized under a high-magnification dark-field microscope. Analysis of the dark-field images shows significantly higher contrast values for anti-HER2 targeted nanoshells compared with the nonspecific IgG targeted nanoshells or untargeted bare nanoshells. HER2-negative MCF 7 cells show significantly less contrast providing additional evidence that enhanced contrast is attributable to the nanoshell binding to SK Br3 cells.

Combined Cancer Imaging and Therapy

Nanoshells have been successfully used for photothermal ablation of cancer cells and for imaging contrast in numerous imaging techniques. It is therefore reasonable to envision a dual diagnostic−therapeutic modality for nanoshells, where the same laser source used for imaging the tumor could at higher laser powers be used to heat and destroy the tumor.

Loo, Lowery, et al.[23] have demonstrated this dual imaging/therapy approach *in vitro* using anti-HER2 immunonanoshells. Nanoshells were designed with a 60 nm core radius, a 10 nm thick shell, and a plasmon resonance at 800 nm. Anti-HER2 or nonspecific anti-IgG were conjugated to nanoshells. SK Br3 breast carcinoma cells were cultured and incubated with immunonanoshells for 1 h. Following rinsing to remove unbound nanoshells, the cells were imaged in a dark-field microscope. Next the cells were irradiated with NIR laser (820 nm wavelength laser 0.008 W/m^2 for 7 min).

Following irradiation the cells were stained and evaluated for nanoshell binding and viability. Figure 5 shows the results of combined imaging and therapy using nanoshells. The controls with no nanoshells or the nonspecific antibody show no contrast in either imaging or therapy. The anti-HER2 nanoshells show a distinct enhancement in the dark-field scattering image and a dark circular area of cell death corresponding to the beam spot upon laser irradiation. The silver stain assay also shows a high density of nanoshells bound to the carcinoma cells.

Gobin et al.[26] have demonstrated *in vivo* imaging via Optical Coherence Tomography (OCT) and therapy using nanoshells. The bifunctional nanoshell designed for the dual role of OCT contrast enhancer and therapeutic heat absorber in tissue has a silica core of 119 nm diameter and a 12 nm gold shell. Mie scattering theory predicts that these particles have approximately 67% of their extinction due to absorption and 33% due to scattering at 800 nm.

Subcutaneously grown tumors in mice (~5 mm in diameter) were injected with PEGylated nanoshells via tail vein injection. The control mice received phosphate buffered solution instead of the nanoshell solution. Twenty hours post injection the tumors were imaged using a commercial OCT setup by applying the probe directly over the tumor touching the skin. Representative OCT images from normal tissue and tumor sites with either PBS or nanoshells are shown in Figure 6. The enhanced brightness in Figure 6, panel D compared with panel C demonstrates that nanoshells provide substantial contrast for OCT imaging. After imaging, the tumors were

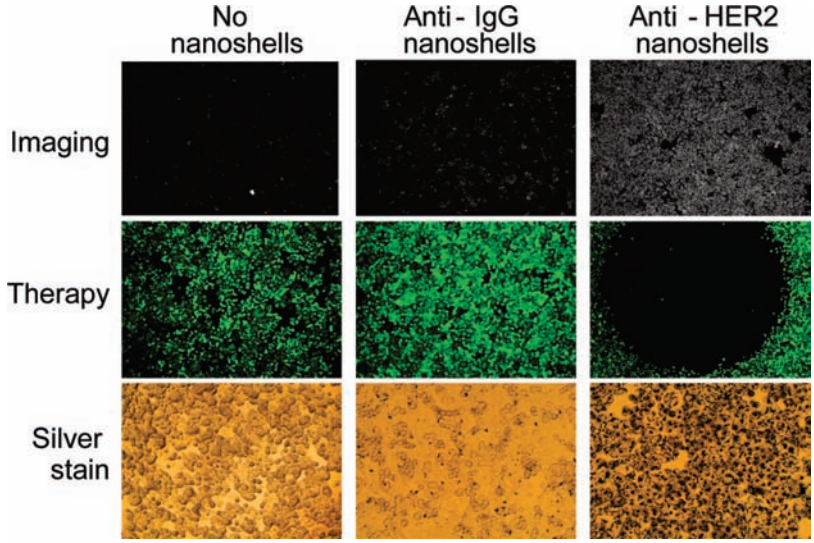

FIGURE 5. Combined imaging and therapy of SKBr3 breast cancer cells using HER2-targeted nanoshells. Scatter-based dark-field imaging of HER2 expression (top row), cell viability assessed via calcein staining (middle row), and silver stain assessment of nanoshell binding (bottom row). Cytotoxicity was observed in cells treated with a NIR-emitting laser following exposure and imaging of cells targeted with anti-HER2 nanoshells only. Figure reproduced with permission from ref 23. Copyright 2005 American Chemical Society.

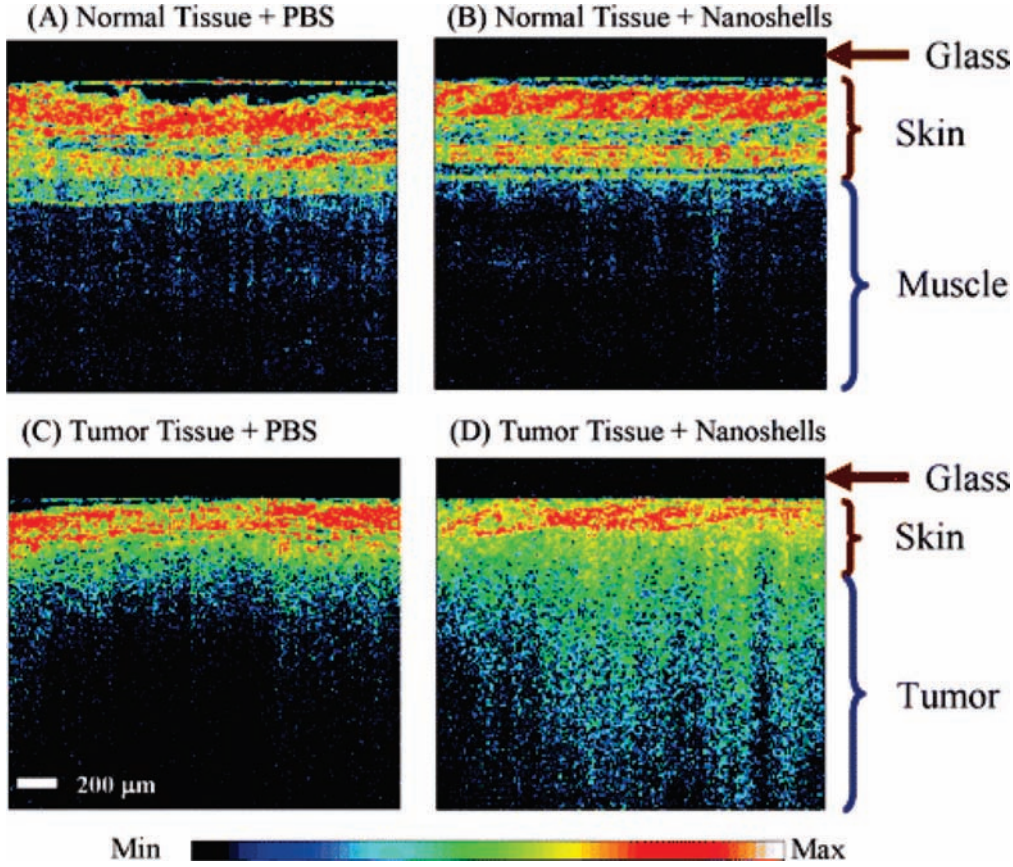

FIGURE 6. Representative OCT images from normal skin and muscle tissue areas of mice systemically injected with PBS (A) or with nanoshells (B). Representative OCT images from tumors of mice systemically injected with PBS (C) or with nanoshells (D). The glass of the probe is 200 μm thick and shows as a dark nonscattering layer. Figure reproduced with permission from ref 26. Copyright 2007 American Chemical Society.

irradiated using a NIR laser (808 nm, 4 W/cm^2, and a spot size of 5 mm) for 3 min. Tumor size and animal survival were monitored for 7 weeks. The median survival for the group receiving sham treatment (laser irradiation with no nanoshells)

was 14 days, while the control group (receiving neither nanoshells nor laser irradiation) was 10 days. The tumors in all but two mice receiving nanoshells and laser treatment had completely regressed in 21 days. Median survival for this group was longer than the 7 weeks of the study period.

Nanoshell Targeting of Tumor Hypoxia

The passive accumulation of nanoshells relies on the EPR effect. However, the centers of large solid tumors are frequently hypoxic, with drastically reduced blood flow. These regions are resistant to nanoparticle accumulation as well as conventional chemotherapy. Since it is believed that these regions are the source of resistant cells which ultimately produce recurrence and metastasis, developing a delivery method for therapeutics to these regions is an important challenge.

Choi et al. have developed a "Trojan Horse" strategy to deliver nanoshells to these hypoxic regions of solid tumors (Figure 7).[31] In response to the presence of hypoxia and necrosis, peripheral blood monocytes enter the tumor due to a chemoattractive gradient. Once inside, the monocytes differentiate into macrophages, which can make up ~70% of the tumor mass. Monocytes loaded with nanoshells are delivered to the tumor periphery where they enter the tumor and differentiate into nanoshell-loaded macrophages. Once distributed inside the tumor mass, irradiation with a NIR laser activates the photothermal destruction of the macrophages and the tumor including the hypoxic regions. Choi et al. have successfully demonstrated several critical steps in this strategy.[31] An in vitro tumor model with a necrotic, hypoxic core was constructed using malignant breast epithelial cells and macrophage loaded with nanoshells, and then irradiated with a pulsed NIR laser (754 nm, 1.54 W total power at source) with varying power at the tumor. Above a certain threshold power, tumor ablation was observed.

The hypoxic regions of the solid tumors are also resistant to traditional treatment modalities. Any strategy to alleviate tissue hypoxia would thus make these aggressive tumors amenable to radiation and chemo- and immunotherapies. One such strategy is mild hyperthermia. Mild hyperthermia allows increased perfusion in the tumor and reduces the hypoxic regions. Although it has been proven in clinical settings that hyperthermia improves the long-term prognosis of radiation therapy, it is underutilized since there are no noninvasive means of achieving local hyperthermia for long periods of time. Diagaradjane et al.[32] have demonstrated the use of nanoshell-mediated hyperthermia as an adjunct to radiation therapy. The nanoshell-induced hyperthermia raises the temperature of the tumors by ~10 °C and allows early perfusion into the tumors, reducing hypoxic regions and leading to necrosis that complements the radiation-induced cell death.

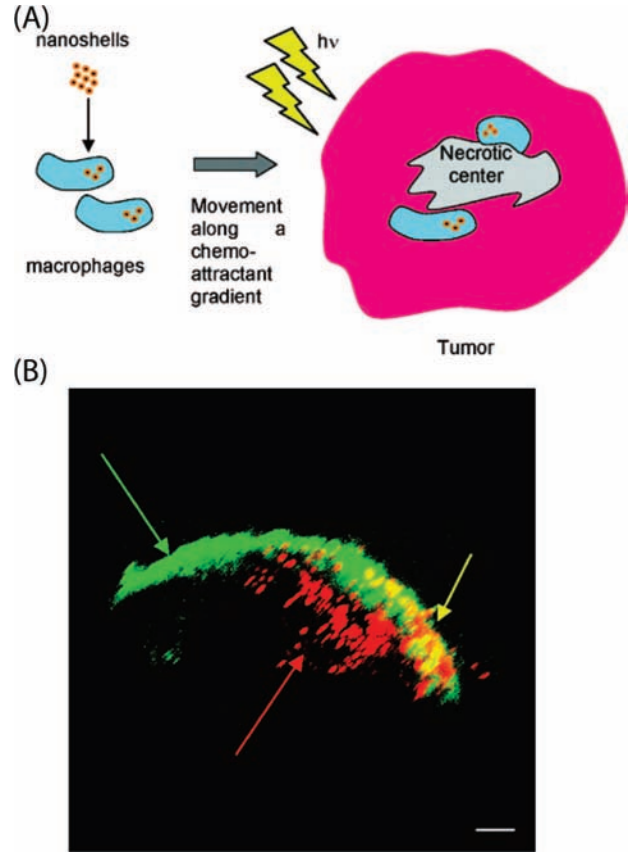

FIGURE 7. (A) Schematic of Trojan Horse therapeutic nanoparticle delivery into hypoxic region of tumor. (B) Frame from three-dimensional reconstruction of tumor spheroid. Viable cells (green fluorescence) form an outer shell around the central necrosis: green arrow, unirradiated cells; red arrow, nanoshell-laden macrophages, which have infiltrated into the area in the center of the spheroid. Yellow cells and arrow may represent cells that have been thermally damaged due to their location next to macrophages. Cells to the left in the photo (green arrow) have not been irradiated, serving as internal control. Scale bar is 50 μm. Figure reproduced with permission from ref 31. Copyright 2007 American Chemical Society.

While nanoshells hold tremendous potential in the single point of care integration of imaging and therapy, currently the technology has a few limitations that need to be addressed as this treatment of cancers moves into clinical settings.[28]

1. Currently there is a need for effective quantification methods for nanoshell accumulation in tumors, which when combined with standard illumination geometries for tumors in specific organs will enable complete regression of tumors.[28]
2. Additional research and accurate theoretical models of concentration profiles for nanoshells in tumors and their achievable temperature elevations are needed to apply this technique as generally as possible to tumor remission.

3. Most of the current *in vivo* studies have been on subcutaneous tumors easily accessible to NIR light applied over the skin surface. NIR light penetration in tissue is a few inches. Techniques to deliver NIR light deep into tissue by exploiting fiber optic probes, for example, need to be applied to this therapeutic modality. Imaging modalities may need to be modified for combined imaging and therapeutics in deep tissue.
4. While these studies seem to demonstrate that the EPR effect occurs in animal models of human tumors,[26,28] almost all of these models use ectopic, that is, subcutaneous, injection of malignant cells in order to form tumors. It is a critically important clinical question to consider how faithfully these models recapitulate human malignancy. Interstitial fluid pressure (IFP) in orthotopic versus subcutaneous human osteosarcoma xenografts has been compared,[33] where the baseline IFP was significantly higher in orthotopic than in subcutaneous tumors of comparable size. Therefore, there may be a net flow of nanoparticles into subcutaneous tumors in animal models but not into orthotopic human tumors.
5. Toxicity concerns need to be addressed in a serious and systematic way. Recent publications, such as the report of carbon nanotubes injected into mice resulting in mesothelioma, contribute to the public's unease.[34,35] It is of paramount importance with every novel application of nanotechnology for the detection and treatment of cancer that efforts be made to identify all potential toxicities, both those to the patient and those to the environment. With this diligent oversight, the unreserved enthusiasm of the public should support this potentially revolutionary endeavor.

The ways in which nanotechnology may enter clinical oncology will only be limited by our imagination. Nanotherapy strategies may function as stand-alone therapy but are also likely to be adjunctive to current systemic therapies. Since nanoshell-based photothermal therapy functions in ways completely different from conventional therapies, its resistance mechanisms are unlikely to be similar. We can ultimately envision utilizing nanoparticles as nanovehicles to deliver therapeutics to sites of disease notoriously difficult to treat, that is, the brain. An almost intractable problem in oncology is the treatment of primary brain malignancies and multiple metastatic deposits within the brain. Nanovehicles engineered to penetrate the blood−brain barrier could be utilized to ferry therapeutics across the barrier. Hypoxic brain tumors (glioblastoma multiforme) may be particularly vulnerable to the macrophage "Trojan Horse" approach.[31]

This work was supported by the Robert A. Welch Foundation Grant C-1220, The U.S. Army Medical Research and Material Command, 820 Chandler Street, Fort Detrick, MD 21702-5014, under Grant No. DAMD17-03-1-0384. Additional funding was provided by grants from the Air Force Office of Scientific Research, The National Science Foundation, National Aeronautics and Space Administration (S.L. and N.J.H.), and the Breast Cancer Research Foundation (S.C.).

BIOGRAPHICAL INFORMATION

Surbhi Lal received her Ph.D. in Applied Physics in 2006 from Rice University. Since 2006, she has been a Postdoctoral Research Associate in the Halas Nanophotonics Group at Rice University. Her research interests are in the area of nanophotonics and surface enhanced spectroscopy.

Susan E. Clare is an Assistant Professor of Surgery at the School of Medicine at Indiana University. Her current interests are the development of the normal breast particularly with regard to the role of progenitor cells, the effect of surgical extirpation of a primary breast cancer on the growth of micrometastatic disease, and the utilization of nanovectors for the treatment of breast cancer.

Dr. Naomi J. Halas is currently The Stanley C. Moore Professor in Electrical and Computer Engineering and Professor of Chemistry, and Bioengineering at Rice University. She is best known scientifically as the inventor of nanoshells. She has subsequently shown numerous applications for nanoshells in biomedicine and in chemical sensing. She is author of more than 150 refereed publications, has ten issued patents, and more than 275 invited talks. She is Fellow of the SPIE, OSA, IEEE, APS, and AAAS.

FOOTNOTES

*To whom correspondence should be addressed. E-mail: halas@rice.edu.

REFERENCES

1 Jemal, A.; Siegel, R.; Ward, E.; Hao, Y.; Xu, J.; Murray, T.; Thun, M. J. Cancer statistics, 2008. *CA: Cancer J. Clin.* **2008**, *58* (2), 71–96.

2 U.S. Census Bureau: Projected Population of the United States, by Age and Sex: 2000 to 2050. http://www.census.gov/ipc/www/usinterimproj/natprojtab02b.pdf.

3 Szabo, L. Cancer burden expected to soar, overwhelm doctors. USA Today March 13, 2007.

4 Bohren, C. F.; Huffman, D. R. *Absorption and Scattering of Light by Small Particles*; John Wiley and Sons, Inc: New York, 1983.

5 Halas, N. J. Playing with Plasmons: Tuning the Optical Resonant Properties of Nanoshells. *MRS Bull.* **2005**, *30*, 362–367.

6 Jain, P. K.; Lee, K. S.; El-Sayed, I. H.; El-Sayed, M. A. Calculated Absorption and Scattering Properties of Gold Nanoparticles of Different Size, Shape, and Composition: Applications in Biological Imaging and Biomedicine. *J. Phys. Chem. B* **2006**, *110*, 7238–7248.

7 Oldenburg, S. J.; Averitt, R. D.; Westcott, S. L. Nanoengineering of Optical Resonances. *Chem. Phys. Lett.* **1998**, *288*, 243–247.

8 Weissleder, R. A Clearer Vision for in Vivo Imaging. *Nat. Biotechnol.* **2001**, *19*, 316–317.

9 Huang, X.; El-Sayed, I. H.; Qian, W.; El-Sayed, M. A. Cancer Cell Imaging and Photothermal Therapy in the Near-Infrared Region by Using Gold Nanorods. *J. Am. Chem. Soc.* **2006**, *128*, 2115–2120.

10 Hu, M.; Chen, J.; Li, Z.-Y.; Au, L.; Hartland, G. V.; Li, X.; Marquez, M.; Xia, Y. Gold Nanostructures: Engineering Their Plasmonic Properties for Biomedical Applications. *Chem. Soc. Rev.* **2006**, *35*, 1084–1094.

11 McDonald, D. M.; Baluk, P. Significance of Blood Vessel Leakiness in Cancer. *Cancer Res.* **2002**, *62*, 5381–5385.

12 Maeda, H. The Enhanced Permeability and Retention (EPR) Effect in Tumor Vasculature: The Key Role of Tumor-Selective Macromolecular Drug Targeting. *Adv. Enzyme Regul.* **2001**, *41*, 189–207.

13 Maeda, H.; Fang, J.; Inutsuka, T.; Kitamoto, Y. Vascular Permeability Enhancement in Solid Tumor: Various Factors, Mechanisms Involved and Its Implications. *Int. Immunopharmacol.* **2003**, *3*, 319–328.

14 Moghimi, S. M.; Muir, I. S.; Ilium, L.; Davis, S. S.; Kolb-Bachofen, V. Coating Particles with a Block Co-polymer (Poloxamine-908) Suppresses Opsonization but Permits the Activity of Dysopsonins in the Serum. *Biochim. Biophys. Acta* **1993**, *1179*, 157–165.

15 Crawford, J. Clinical Uses of Pegylated Pharmaceuticals in Oncology. *Cancer Treat. Rev.* **2002**, (Suppl. A), 7–11.

16 Lowery, A. R.; Gobin, A. M.; Day, E. S.; Halas, N. J.; West, J. L. Immunonanoshells for Targeted Photothermal Ablation of Tumor Cells. *Int. J. Nanomed.* **2006**, *1*, 1–6.

17 Arap, W.; Pasqualini, R.; Ruoslahti, E. Cancer Treatment by Targeted Drug Delivery to Tumor Vasculature in a Mouse Model. *Science* **1998**, *279*, 377–380.

18 Elliott, A. M.; Stafford, R. J.; Schwartz, J.; Wang, J.; Shetty, A. M.; Bourgoyne, C.; O'Neal, P.; Hazle, J. D. Laser-Induced Thermal Response and Characterization of Nanoparticles for Cancer Treatment Using Magnetic Resonance Thermal Imaging. *Med. Phys.* **2007**, *34*, 3102–3108.

19 James, W. D.; Hirsch, L. R.; West, J. L.; O'Neal, P. D.; Payne, J. D. Application of INAA to the Build-up and Clearance of Gold Nanoshells in Clinical Studies in Mice. *J. Radioanal. Nucl. Chem.* **2007**, *271*, 455–459.

20 Xie, H.; Gill-Sharp, K. L.; O'Neal, D. P. Quantitative Estimation of Gold Nanoshell Concentrations in Whole Blood Using Dynamic Light Scattering. *Nanomedicene* **2007**, *3*, 89–94.

21 Hirsch, L. R.; Stafford, R. J.; Bankson, J. A.; Sershen, S. R.; Rivera, B.; Price, R. E.; Hazle, J. D.; Halas, N. J.; West, J. L. Nanoshell-Mediated Near-Infrared Thermal Therapy of Tumors under Magnetic Resonance Guidance. *Proc. Natl. Acad. Sci. U.S.A.* **2003**, *100* (23), 13549–13554.

22 Loo, C.; Lin, A.; Hirsch, L.; Lee, M.-H.; Barton, J.; Halas, N.; West, J.; Drezek, R. Nanoshell-Enabled Photonics-Based Imaging and Therapy of Cancer. *Technol. Cancer Res. Treat.* **2004**, *3*, 33–40.

23 Loo, C.; Lowery, A.; Halas, N.; West, J.; Drezek, R. Immunotargeted Nanoshells for Integrated Cancer Imaging and Therapy. *Nano Lett.* **2005**, *5* (4), 709–711.

24 Zaman, R. T.; Diagaradjane, P.; Wang, J. C.; Schwartz, J.; Rajaram, N.; Gill-Sharp, K. L.; Cho, S. H.; Rylander, H. G. I.; Payne, J. D.; Krishnan, S.; Tunnell, J. W. In Vivo Detection of Gold Nanoshells in Tumors Using Diffuse Optical Spectroscopy. *IEEE J. Sel. Top. Quantum Electron.* **2007**, *13*, 1715–1720.

25 Wang, Y.; Xie, X.; Wang, X.; Ku, G.; Gill, K. L.; O'Neal, D. P.; Stoica, G.; Wang, L. V. Photoacoustic Tomography of a Nanoshell Contrast Agent in the in Vivo Rat Brain. *Nano Lett.* **2004**, *4*, 1689–1692.

26 Gobin, A. M.; Lee, M. H.; Halas, N. J.; James, W. D.; Drezek, R. A.; West, J. L. Near-Infrared Resonant Nanoshells for Combined Optical Imaging and Photothermal Cancer Therapy. *Nano Lett.* **2007**, *7*, 1929–1934.

27 O'Neal, D. P.; Hirsch, L. R.; Halas, N. J. D. P. J.; West, J. L. Photo-thermal Tumor Ablation in Mice Using near Infrared-Absorbing Nanoparticles. *Cancer Lett.* **2004**, *209*, 171–176.

28 Stern, J. M.; Stanfield, J.; Kabbani, W.; Hsieh, J.-T.; Cadeddu, J. A. Selective Prostate Cancer Thermal Ablation With Laser Activated Gold Nanoshells. *J. Urol.* **2008**, *179*, 748–753.

29 Loo, C.; Hirsch, L.; Lee, M.-H.; Chang, E.; West, J.; Halas, N.; Drezek, R. Gold Nanoshell Bioconjugates for Molecular Imaging in Living Cells. *Opt. Lett.* **2005**, *30*, 1012–1014.

30 Park, J.; Estrada, A.; Sharp, K.; Sang, K.; Schwartz, J. A.; Smith, D. K.; Coleman, C.; Payne, J. D.; Korgel, B. A.; Dunn, A. K.; Tunnell, J. W. Two-Photon-Induced Photoluminescence Imaging of Tumors Using near-Infrared Excited Gold Nanoshells. *Opt. Express* **2008**, *16*, 1590–1599.

31 Choi, M.-R.; Stanton-Maxey, K. J.; Stanley, J. K.; Levin, C. S.; Bardhan, R.; Akin, D.; Badve, S.; Sturgis, J.; Robinson, J. P.; Bashir, R.; Halas, N. J.; Clare, S. E. A Cellular Trojan Horse for Delivery of Therapeutic Nanoparticles into Tumors. *Nano Lett.* **2007**, *7*, 3759–3765.

32 Diagaradjane, P.; Shetty, A.; Wang, J. C.; Elliott, A. M.; Schwartz, J.; Shentu, S.; Park, H. C.; Deorukhkar, A.; Stafford, R. J.; Cho, S. H.; Tunnell, J. W.; Hazle, J. D.; Krishnan, S. Modulation of in Vivo Tumor Radiation Response via Gold Nanoshell-Mediated Vascular-Focused Hyperthermia: Characterizing an Integrated Antihypoxic and Localized Vascular Disrupting Targeting Strategy. *Nano Lett.* **2008**, *8*, 1492–1500.

33 Brekken, C.; Bruland, O. S.; de Lange Davies, C. Interstitial Fluid Pressure in Human Osteosarcoma Xenografts: Significance of Implantation Site and the Response to Intratumoral Injection of Hyaluronidase. *Anticancer Res.* **2000**, *20* (5B), 3503–3512.

34 Poland, C. A.; Duffin, R.; Kinloch, I.; Maynard, A.; Wallace, W. A. H.; Seaton, A.; Stone, V.; Brown, S.; MacNee, W.; Donaldson, K. Carbon nanotubes introduced into the abdominal cavity of mice show asbestos-like pathogenicity in a pilot study. *Nat. Nanotechnol.* **2008**, *3*, 423–428.

35 Takagi, A.; Hirose, A.; Nishimura, T.; Fukumori, N.; Ogata, A.; Ohashi, N.; Kitajima, S.; Kanno, J. Induction of mesothelioma in p53± mouse by intraperitoneal application of multi-wall carbon nanotube. *J. Toxicol. Sci.* **2008**, *33* (1), 105–116.